Teleoperation of a Robot Manipulator using EMG Signals and a Position Tracker

Panagiotis K. Artemiadis and Kostas J. Kyriakopoulos

Control Systems Lab, Mechanical Eng. Dept.
National Technical University of Athens
9 Heroon Polytechniou Str, Athens, 157 80, Greece

{partem, kkyria}@mail.ntua.gr

***Abstract* – A methodology for a robotic manipulator teleoperation is presented. The proposed method can realize a new master-slave manipulator system that uses no mechanical master controller but electromyographic (EMG) signals from the muscles of a human arm. EMG signals are acquired from biceps brachii, main responsible muscle for elbow flexion. The robot elbow is controlled using joint angle computed from EMG signal during smooth forearm motion, while the shoulder of the robot is controlled by a position tracker placed on the user's arm. Identification techniques are used to approximate the user-dependent parameters of the model used to compute the elbow angle based on EMG signals.**

Index Terms* – *electromyographic (EMG) signal, robot teleoperation, parameter identification.

I. Introduction

Teleoperation of robots has received increased attention in the last years. The interest is motivated by the large variety of applications in remote or dangerous environments. Lately there is an increasing demand for direct and more natural means of interface between the user and the teleoperated robot. Specifically, the user's motion should not be impeded by complicated interface sensors or machinery. Moreover, a lot of applications demand that the user's motion should be generated by natural movements of human upper limb and not by un-natural and wearing motion. The use of electromyographic (EMG) signals as the master-slave interface has the advantage of being both convenient and natural for the master. Furthermore an amputee-user, who has lost a part of the upper limb, will have the ability to teleoperate a robotic manipulator for daily activities, using EMG signals if the central nervous system and a part of the muscles that actuated the original limb still exist after amputation.

Many applications concerning prosthetic or orthotic devices have used EMG signals as control signals. Concerning prosthetic devices, EMG signals have often been used as control signals, such as the Waseda hand [1], the Boston arm [2], and the Utah artificial arm [3]. Orthotic devices such as arm exoskeletons have also been developed and controlled using EMG signals [4]. Many studies on EMG signal pattern discrimination methods have been proposed in order to extract the user intended motion. Linear prediction models and pattern discrimination methods using neural networks [6] have been proposed in the past for this scope. Teleoperation of a robot arm using EMG signals was firstly introduced successfully by Fukuda [5]. It was the first attempt to integrate EMG signal with a position tracking system in order to teleoperate a robotic arm. He has developed an EMG pattern discrimination algorithm for computing the intention of the user regarding his/her wrist movement, while the manipulator was controlled by a position tracking system.

In this paper, an integrated system composed by EMG signal acquisition and a position tracker is used to drive a robotic manipulator. EMG signals from biceps brachii are used to drive the elbow joint of the robotic arm, while a position tracker is placed on the user's arm to drive the shoulder joints of the manipulator. The robotic manipulator used is a 7- degrees of freedom (DOFs) Mitsubishi Heavy Industries PA-10 (Fig. 1). A Hill type of model is adopted to represent the mechanical model of the recorded muscle [7]. Parameter identification techniques are used to estimate the Hill model parameters which are user-dependent. From this model, the user applied torque can be estimated. Furthermore, using a simplified dynamic model of the forearm and wrist parts of the user's upper limb, the elbow joint angle can be estimated. The parameters of this dynamic model are also estimated by the identification algorithm. Then, the estimated elbow joint angle is used to drive the corresponding joint of the robotic arm. Using the position tracker, the shoulder joints of the manipulator are also driven. So the main contribution of the paper is the modeling of musculo-skeletal dynamics in order to compute elbow joint angle by using only EMG signals from biceps brachii. It must be noted that the user's elbow motion is smooth and is limited in flexion-extension.

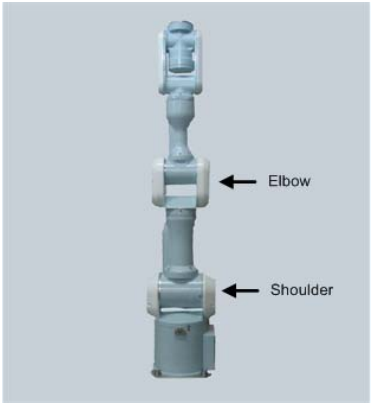

Fig. 1 The PA-10 7-DOFs manipulator and its joints corresponding to the human shoulder and elbow.

The rest of the paper is organized as follows: Section II gives a description of the methodology proposed regarding elbow and shoulder joints, with the appropriate segregation of the distributed sub-problems. Section III illustrates the efficiency of the approach through a number of experimental results, while section IV concludes the paper.

II. METHODOLOGY

We consider two parts of the robotic manipulator to be driven. The elbow will be driven by EMG signals from biceps brachii. The shoulder joints will be driven by the position tracking system. This section will describe in details each part.

A. Elbow Joint

Biceps brachii is selected as the main responsible muscle for elbow flexion, in a fully supinated forearm. The block diagram for computing the elbow joint angle from EMG signal from biceps brachii is depicted on Fig. 2.

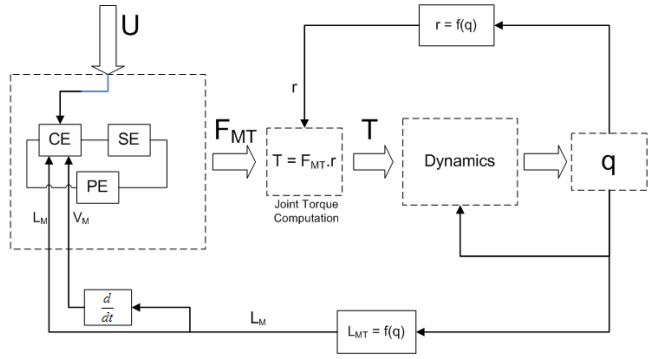

Fig. 2 The elbow controller block diagram

Musculo-sceletal modeling

The EMG signal, after preliminary processing, it is used as input (U) to the Hill model of the corresponding muscle. The Hill model provides a simplified representation of skeletal muscles and many researchers have contributed to its development. The used formulation of the Hill-based model is a synthesis of ideas and mathematical expressions from several references. The most consistent source of that model has been proposed by Winters [8]. The model consists of three elements, as shown on Fig. 3: a contractile element (CE), a series element (SE) and a parallel element (PE).

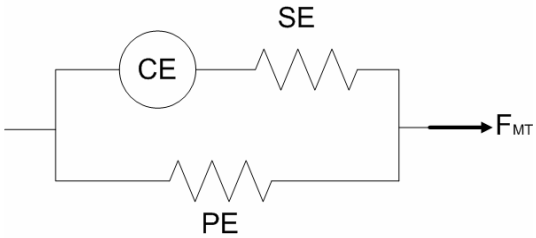

Fig. 3 The Hill-based muscle model

The SE and PE components represent passive soft connective tissue including the tendon and the non-active muscle fibers. The force-extension relations of these elements are defined [4] by:

$$F_{SE} = \frac{F_{SE_{\max}}}{e^{SE_{sh}} - 1}\left(e^{SE_{sh} \cdot dL_{SE} / dL_{SE_{\max}}} - 1\right) \quad (1)$$

$$F_{PE} = \frac{F_{PE_{\max}}}{e^{PE_{sh}} - 1}\left(e^{PE_{sh} \cdot dL_{PE} / dL_{PE_{\max}}} - 1\right) \quad (2)$$

where F_{SE} , dL_{SE} and F_{PE} , dL_{PE} are the forces and extensions of elements *SE* and *PE* respectively, while subscript "max" indicates maximum values. SE_{sh} and PE_{sh} are the SE and PE shape parameters.

The CE component represents the active muscle fibers. It acts as a force generator and has two basic properties that characterize it: the force-length and the force-velocity relation. The force generated by this component depends not only on these two relations, but on the muscle activation too. Muscle activation is generally defined as the quantity of the recruited muscle fibers for a specific task, and is depicted at the EMG recording. A typical muscle activation form of the biceps brachii during elbow flexion as depicted in raw and processed EMG recording is shown on Fig. 4.

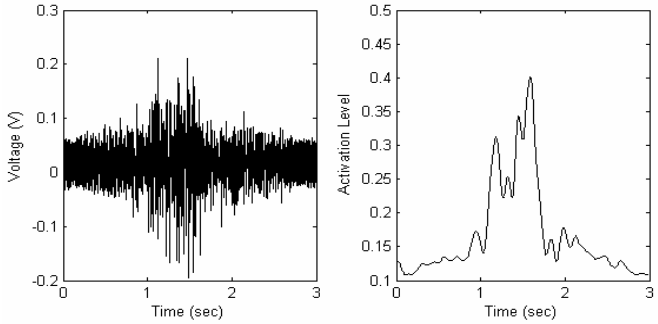

Fig. 4 Typical raw EMG signal and corresponding activation level

Thus, the total force generated by the CE component is defined as a product relationship of the dimensionless force-length and force-velocity functions $f_{FL}\left(L_{CE}\right)$ and $f_{FV}\left(V_{CE}\right)$ respectively, the activation level U and a gain factor representing the maximum generated force $F_{CE_{\max}}$:

$$F_{CE} = f_{FL}\left(L_{CE}\right) \cdot f_{FV}\left(V_{CE}\right) \cdot F_{CE_{\max}} \cdot U \quad (3)$$

Functions $f_{FL}\left(L_{CE}\right)$ and $f_{FV}\left(V_{CE}\right)$ are:

$$f_{FL} = e^{-0.5\cdot\left(\frac{L_{CE}/L_0 - 1.05}{0.19}\right)^2} \quad (4)$$

$$f_{FV} = \frac{0.1433}{0.1074 + e^{-1.409\cdot\sinh\left(3.2 V_{CE}/V_{\max} + 1.6\right)}} \quad (5)$$

where L_{CE} and L_0 are the length and resting length of the CE component, V_{CE} is the shortening velocity of the CE component, and V_{max} is the maximum velocity of this component, which depends on the activation level U and the velocity V_0 [8] at the muscle fiber resting length

$$V_{\max} = 0.5\left(U + 1\right)V_0 \quad (6)$$

One assumption that can be made about the examined muscle is that, due to the large stiffness of the SE representing the tendon, it can be regarded as a non-deformable element,

without imposing large errors [9]. Thus, the total force F_{MT} applied by the examined muscle is

$$F_{MT} = F_{CE} + F_{PE} \quad (7)$$

The relation of the lengths of the three components with respect to the total musculotendon length L_{MT} is

$$L_{MT} = L_{PE} = L_{CE} + L_{SE} = L_{CE} + L_S \quad (8)$$

where L_S is called the slack length of the tendon, which according to the assumption made above $L_S = const$.
Pigeon [10] estimated the total musculotendon length using a fourth order polynomial of corresponding joint angle q_e

$$L_{MT} = a_0 + a_1 q_e + a_2 q_e^2 + a_3 q_e^3 + a_4 q_e^4 \quad (9)$$

where a_i, $i = 0, \ldots, 4$, are coefficients found in [10]. This equation is scaled for each user only for a_0, due to the fact that muscle origin and insertion point are same for each user, and are specifically defined in anatomy. The elbow angle q_e and the musculotendon length L_{MT} are depicted on Fig. 5.

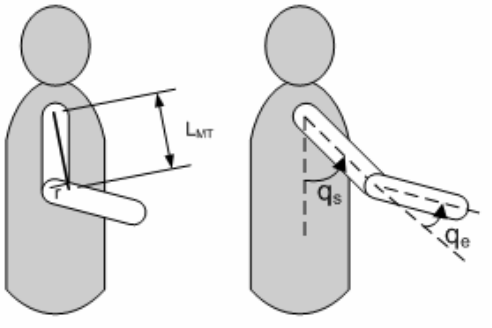

Fig. 5 Total muscle length, elbow and shoulder angle

As shown on Fig. 5, to compute the applied torque we need distance r, called the muscle moment, and defined as the length of the vector perpendicular to the force vector, with origin at the joint center. It is dependent on musculoskeletal morphology and related with joint angle q_e by

$$r = b_0 + b_1 q_e + b_2 q_e^2 + b_3 q_e^3 + b_4 q_e^4 + b_5 q_e^5 \quad (10)$$

where b_i, $i = 0,\ldots, 4$, are found in [10]. The applied joint torque T is then

$$T = F_{MT} \cdot r \quad (11)$$

Dynamic modeling

As shown on Fig. 2, the applied torque T acts as input to the dynamic model of the forearm and hand of the user. A single-link dynamic model of that part of the upper limb is

$$T = \left(I + md^2\right)\ddot{q}_e + mgd\sin\left(q_e + q_s\right) \quad (12)$$

where I is the total moment of inertia with respect to the rotation axis, m the total mass of the forearm and hand, q_e the elbow angle, q_s the shoulder angle and g the gravity acceleration. The distance d between the total center of mass of the forearm and hand is

$$d = \left(m_f l_f + m_h l_h\right)\Big/ m_f + m_h \quad (13)$$

where m_f, m_h are the masses of forearm and hand respectively and l_f, l_h the distances of their individual centers of mass from the elbow joint. The total moment of inertia I can be found using Steiner's theorem and the individual moments of inertia of the forearm and hand.

Parameter Identification

The user elbow angle can be estimated by numerically integrating (12), in conjunction to (1-7, 11), if the initial value of joint angle q_e is known.

This model is highly based on some parameters that are user-dependent. A parameter estimation method based on identification techniques is proposed to adjust these parameters on each user. This fact presupposes a calibration phase, in which the user executes a small number of pre-described motions consisting of elbow flexion/extension. During these motions, the position tracker is placed on user's forearm in order to monitor the forearm position and compute the elbow joint angle.

Making use of the total model described above and all the assumptions made, the parameters to be identified are presented in Table I.

TABLE I
MODEL PARAMETERS TO BE IDENTIFIED

Parameters	
θ_1	F_{PEmax}
θ_2	PE_{sh}
θ_3	L_0
θ_4	F_{CEmax}
θ_5	L_S
θ_6	I
θ_7	m
θ_8	d

The parameter estimation method is realized via optimization. If $q_d(t)$ are the monitored values of the human elbow joint and $q_e(t)$ are the elbow joint angle estimate, then an objective function f is defined

$$f = \sum_{i=1}^{n}\left(q_d\left(\left(i + i_d\right)\cdot\Delta\mathrm{T}\right) - q_e\left(i\cdot\Delta\mathrm{T}\right)\right)^2 - k \quad k > 0 \quad (14)$$

where n the number of the angle positions estimated by the model, k a real number adjusting the acceptable error in the model output, ΔT the time interval between the discrete values compared and i_d a factor accounting for the delay between the measured angle and that computed by the model at time $i\cdot\Delta T$. Note also that $q_e(t)$, $q_d(t)$ are measured in rad.

The parameter vector θ is subject to constraints deriving either from musculoskeletal geometry e.g. θ_3, θ_5, θ_8, or physical constraints e.g. θ_1, θ_2, θ_6, θ_7. The constraints are:

$$\begin{aligned} \theta_1 > 0 \qquad & \theta_6 > 0 \\ 0 < \theta_2 < 15 \qquad & \theta_7 > 0 \\ L_{MT\min} < \theta_3 + \theta_5 < L_{MT\max} \qquad & 0 < \theta_8 < 1 \end{aligned} \quad (15)$$

Optimization is realized by sequential quadratic programming (SQP) implemented by the built-in function of the software package Matlab™ 6.5. The initial estimate of the parameter vector θ is based on values found in literature [8-10]. The typical number of iterations needed for the algorithm to converge is 80.

B. Shoulder Joints

The shoulder is driven by a methodology based on a 3-D position tracking sensor (Isotrak II, Polhemus Inc.) placed on the arm of the user, as close as possible to the elbow joint. Electromagnetic fields are used to determine its 3-D position with respect to a reference frame placed in a firm place near the user. To achieve system portability, we do not necessarily require that the initial user arm position is pre-specified.

Within the same framework, the tracker point is corresponded to a point coinciding with a joint of the robotic arm (elbow joint). Thus, the driving command for the shoulder joints of the robotic arm is the relative displacement of the position tracker wrt to its initial position. The coordinate frames of the tracking system and the robotic arm, along with the corresponding points, are shown on Fig. 6.

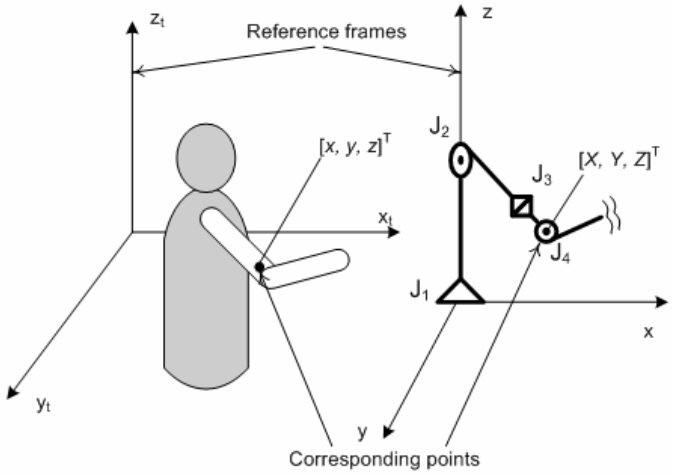

Fig. 6. The coordinate systems and corresponding points

Thus, given a displacement $[dx\ dy\ dz]^T$ of the tracking sensor expressed to the tracker coordinate frame, the displacement $[dX\ dY\ dZ]^T$ of the corresponding point on the robotic elbow expressed wrt the robotic reference frame will be

$$\begin{bmatrix} dX \\ dY \\ dZ \end{bmatrix} = \mathbf{k} \cdot \begin{bmatrix} dx \\ dy \\ dz \end{bmatrix} = \begin{bmatrix} k_x & 0 & 0 \\ 0 & k_y & 0 \\ 0 & 0 & k_z \end{bmatrix} \cdot \begin{bmatrix} dx \\ dy \\ dz \end{bmatrix} \tag{16}$$

where $\boldsymbol{k}$ is a gain matrix regulating the sensitivity of the robotic arm motion wrt the user's motion. The accumulated errors are minimized by checking the absolute position of the sensor with respect to its initial position, when the user's arm is not moving.

If before the displacement of the robotic manipulator the corresponding point on the robotic elbow was at $[X_0\ Y_0\ Z_0]^T$, its new position will be

$$\begin{bmatrix} X & Y & Z \end{bmatrix}^T = \begin{bmatrix} X_0 & Y_0 & Z_0 \end{bmatrix}^T + \begin{bmatrix} dX & dY & dZ \end{bmatrix}^T \tag{17}$$

Since (see appendix)

$$\begin{aligned} \mathrm{X} &= 0.45\cos(q_1)\sin(q_2) \\ Y &= 0.45\sin(q_1)\sin(q_2) \\ Z &= 0.317 + 0.45\cos(q_2) \end{aligned} \tag{18}$$

the angles q_1, q_2, q_3 of the J_1, J_2, J_3 joints of the robotic manipulator required are computed by inverse kinematics:

$$\begin{aligned} q_1 &= Arc\tan 2\left(\frac{Y}{0.45\sin(q_2)}, \frac{X}{0.45\sin(q_2)}\right) = \\ &= Arc\tan 2(Y, X) \\ q_2 &= Arc\tan 2\left(\pm\frac{1}{0.45}\sqrt{X^2+Y^2}, \frac{Z-0.317}{0.45}\right) = \\ &= Arc\tan 2\left(\pm\sqrt{X^2+Y^2}, Z-0.317\right) \end{aligned} \tag{19}$$

It must be noted that:

- Eq. (19) is valid when $q_2 \neq 0, \pi$. If $q_2 = 0$ or π, the elbow point position $[X\ Y\ Z]^T$ is not related to joint angle q_1 and the shoulder can not be moved in space.
- The negative solution of q_2 is always selected in order to comply with robot's joint limits for angle q_1.
- The angle of joint J_3 does not affect the elbow position and thus remains at its initial position.

C. Implementation Issues

One issue that must be analyzed is the effect of the user's arm configuration on the recorded EMG signal from biceps brachii. We have observed that the shoulder angle affects the EMG activation level of biceps brachii, while the elbow joint is still at zero position. The effect only concerns activation level magnitude but is of much importance because it would affect the muscle model too.

To alleviate that, we propose a pattern discrimination algorithm. This algorithm is based on the fact that the EMG activation level, while the elbow joint is still, is scaled as shoulder angle is increasing. Despite that, the amplitude of the muscle activation can not be computed based on the shoulder configuration. The proposed algorithm is based on the fact that the flexion of the elbow causes a distinguishable change in muscle activation. That is briefly characterized by a peak value that holds for a quite enough number of samples. We consider the cost function

$$G(m) = \sum_{i=m-n}^{n}\left[\dot{U}(i\cdot\Delta\mathrm{T})\cdot\left(U(i\cdot\Delta\mathrm{T}) - \left(\sum_{k=0}^{k=m}U(k\cdot\Delta\mathrm{T})\Big/m\right)\right)\right] - h \tag{20}$$

where $U(i\cdot\Delta T)$ is the muscle activation at discrete time points, ΔT the sampling time interval, m the sample index, n defines a moving window, and h is a tolerance to activation change parameter. Then a satisfactory criterion to distinguish muscle activation caused by elbow flexion from this caused by shoulder motion, is

$$\left|G(m)\right| < \varepsilon \tag{21}$$

where ε a small constant.

III. Experiments

A. System Components

The robotic arm used is a 7-DOF manipulator (PA-10, Mitsubishi Heavy Industries). The control program is developed on a personal computer (Pentium 3, 1.0 GHz)

which communicates with the robot controller through a motion control card and optical fiber interface. The 3D position tracker (Isotrak II, Polhemus Inc.) communicates with the personal computer at a frequency of 60 Hz, through serial communication (RS-232). The size of the position sensor is 2.83(W) 2.29(L) 1.52(H) cm, and sufficiently portable for the user. The static accuracy is ±2.4 mm for axis x, y, z.

Another PC (Pentium 4, 3.2 GHz) is dedicated to the elbow control part. Using a signal acquisition board (NI-DAQ 6036E) we collect EMG signal through an EMG system (Bagnoli-16, Delsys Inc.). Single differential surface EMG electrodes (DE-2.1, Delsys Inc.) are used for recording. The processing of the signal and the elbow control part is performed at this computer. The two subsystems are connected through serial communication (RS-232) for exchanging necessary data. The integrated system is depicted on Fig. 7.

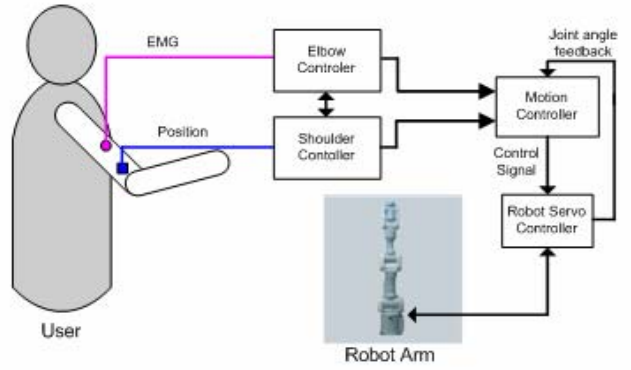

Fig. 7 Total system

B. *Experimental Results*

The operation of the system is divided in two parts: the calibration phase, and the normal operation phase. During both phases, the EMG signal was pre-amplified with a gain factor of 1000 and sampled at 1.0 KHz. Then it was full-wave rectified and filtered through a 4th order Butterworth filter with a cut off frequency of 6 Hz. Then the signal was normalized to its corresponding value recorded through maximum voluntary isometric contraction of the biceps brachii. The experiments conducted with three subjects with fully functional upper limbs. All subjects were within 22-25 years old, body weight 80-95 Kg and height 1.75-1.86 m.

During the calibration phase each subject was asked to perform a smooth flexion/extension of the elbow. Furthermore, the EMG signal at maximum voluntary isometric contraction of biceps brachii and the signal while the arm was still at vertical and horizontal position were recorded. During the smooth flexion/extension of the elbow, the position of the forearm was recorded using the position tracking system, with the sensor placed at the subject's forearm. From these measurements the elbow joint angle $q_d(t)$ was calculated. Those data were compared with that calculated by the model $q_e(t)$ in order to form the objective function defined in (14). The initial values for the parameters of the model to be identified, as listed in Table I, were taken from literature. For subject A, the identification problem converged to a vector after 88 iterations. In Fig. 8, the final value for each of these parameters is compared to its initial value through normalization with respect to initial values.

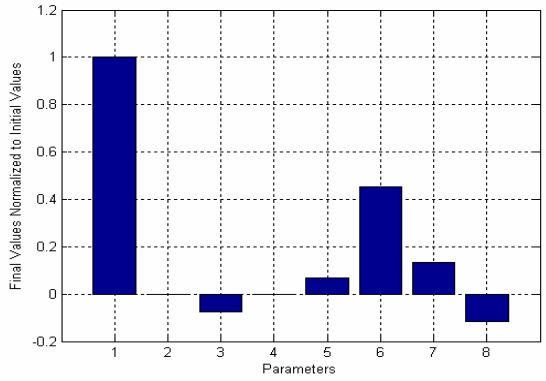

Fig. 8 Initial to final parameter values

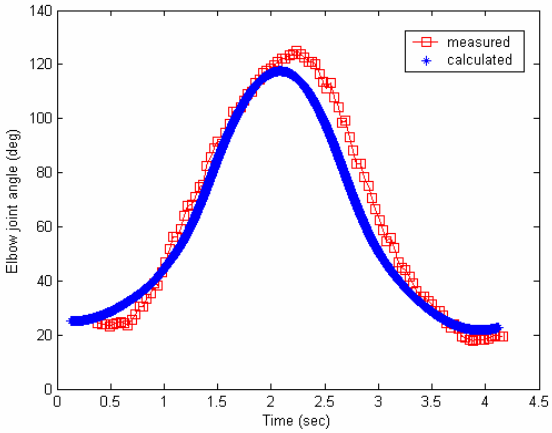

Fig. 9 Elbow joint angle

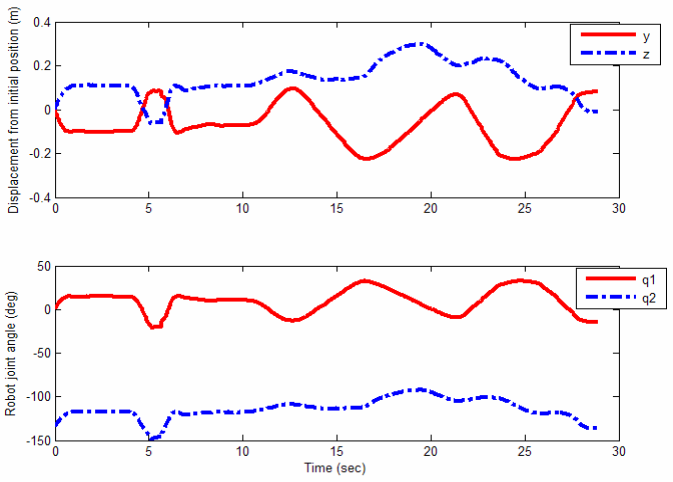

Fig. 10 Shoulder input and output.

During the normal operation phase the subject A was told to move his shoulder according to his will, and also to make smooth flexion/extensions of his elbow, keeping his forearm fully supinated. At system initialization the subject was told to move his arm at an initial position, just to correlate it with the initial position of the robotic manipulator. That position was fully extended elbow, and flexed shoulder at 90 degrees.

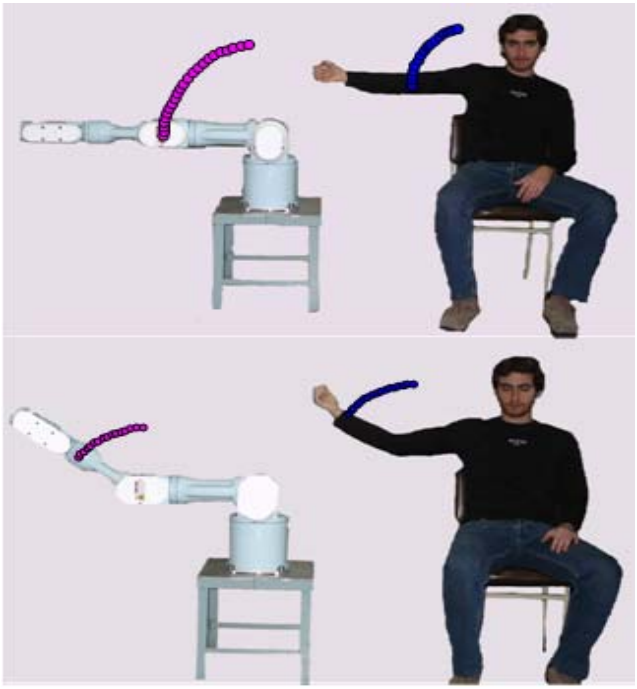

Fig. 11 User and robot trajectories during arm and shoulder motion

After the system initialization, the user performed smooth shoulder and elbow motions as previously described for a period of 30 seconds. The calculated from the model and the actual measured elbow joint angle during a flexion/extension of the subject's elbow are compared on Fig. 9. Displacement measured from the tracking system and corresponding robot joint angles (q_1, q_2) are shown on Fig. 10. Fig. 11 depicts the path followed by both subject and manipulator's arm and forearm during a part of the system operation.

IV. Conclusion

This paper proposes an integrated system that uses signals coming from both human muscles and artificial sensors to drive a robotic manipulator. The controller developed incorporates EMG signals, human arm dynamics and parameter identification techniques in order to drive the robotic arm according to user's intention. Experiments conducted show the robustness of the system in smooth elbow movements.

In our future research, the elbow control part would be further tested in non-smooth movements. The pattern discrimination algorithm developed would be re-assessed and expanded to other kinds of factors that cause EMG signal alteration. The expansion of the total system to other human DOFs (e.g. elbow pronation-supination, wrist flexion-extension) is a future objective too. We would also examine human joint impedance in relation to muscular contraction level, and introduce it to the developed system.

V. Acknowledgment

The authors want to acknowledge the contribution of the European Commission through contract NEUROBOTICS (FP6-IST-001917) project.

Appendix

We define three successive coordinate frames at the center of the rotation axes of the first three joints of the PA-10 manipulator. The homogeneous matrix relating two successive coordinate frames {i-1}-{i}, is given by

$$T_{i-1}^{i}=\begin{bmatrix}\cos q_i & -\cos\alpha_i \sin q_i & \sin\alpha_i \sin q_i & a_i \cos q_i\\ \sin q_i & \cos\alpha_i \cos q_i & -\sin\alpha_i \cos q_i & a_i \sin q_i\\ 0 & \sin\alpha_i & \cos\alpha_i & d_i\\ 0 & 0 & 0 & 1\end{bmatrix} \quad (A.1)$$

Using the PA-10 Denavit-Hartenberg parameters (Table II),

TABLE II
D-H Parameters for the first 3 joints-links of PA-10

α_i (rad)	a_i (m)	d_i (m)
- π/2	0	0.317
+ π/2	0	0
- π/2	0	0.45

the total transformation matrix relating the elbow of the robotic manipulator with the base coordinate system {0} is given by

$$T_0^3 = T_0^1 \cdot T_1^2 \cdot T_2^3 \quad (A.2)$$

where {1}, {2}, {3} the successive coordinate frames. The coordinate frame {3} coincides with the elbow point and the position of this point wrt the base coordinate frame is given by the first three elements of the fourth column of T_0^3 :

$$\begin{bmatrix}X\\Y\\Z\end{bmatrix}=\begin{bmatrix}T_0^3(1,4)\\T_0^3(2,4)\\T_0^3(3,4)\end{bmatrix}=\begin{bmatrix}0.45\cos(q_1)\sin(q_2)\\0.45\sin(q_1)\sin(q_2)\\0.317+0.45\cos(q_2)\end{bmatrix} \quad (A.3)$$

References

[1] Kato, E. Okazaki, H. Kikuchi, and K. Iwanami, "Electropneumatically controlled hand prosthesis using pattern recognition of myo-electric signals," in *Dig. 7th ICMBE*, 1967, pp. 367–367.

[2] R. B. Jerard, T.W.Williams, and C.W. Ohlenbusch, "Practical design of an EMG controlled above elbow prosthesis," in *Proc. Conf. Engineering Devices for Rehabilitation*, Boston, MA, 1974, pp. 73–73.

[3] S. C. Jacobson, D. F. Knutti, R. T. Johnson, and H. H. Sears, "Development of the Utah artificial arm," *IEEE Trans. Biomed. Eng.*, vol. BME-29, pp. 249–269, Apr. 1982.

[4] J. Rosen, M. Brand, M.B. Fuchs, and M. Arcan, "A myosignal-based powered exoskeleton system," IEEE Trans. Systems, Man, and Cybernetics – Part A, vol. 31, no. 3, pp. 210-222, May 2001.

[5] O. Fukuda, T. Tsuji, M. Kaneko, and A. Otsuka, "A human-assisting manipulator teleoperated by EMG signals and arm motions," IEEE Trans. Robotics and Automation, vol 19, no. 2, pp. 210-222, April 2003.

[6] R. J. Triolo and G. D. Moskowitz, "The theoretical development of a multichannel time-series myoprocessor for simultaneous limb function detection and muscle force estimation," *IEEE Trans. Biomed. Eng.*, vol. 36, pp. 1004–1017, Oct. 1989.

[7] A. V. Hill, "The heat of shortening and the dynamic constants of muscle," *Proc. R. Soc. Lond. Biol.*, vol. 126, pp. 136–195, 1938.

[8] J. M. Winters, and L. Stack, "Estimated mechanical properties of synergistic muscle involved in movements of a variety of human joints," *J. Biomech., vol* 21, no 12, 1027–1041, 1988.

[9] F.E. Zajac, "Muscle and tendon: properties, models, scaling, and application to biomechanics and motor control," Crit. Rev. Biomed. Eng. vol 17, pp. 359 – 411, 1989.

[10] P. Pigeon, L. Yashia, and A.G. Feldman, "Moment arms and lengths of human upper limb muscles as functions of joint angles," J. Biomechanics, vol 29, no. 10, pp 1365 – 1370, 1996.